

Threshold pion production in heavy-ion collisions*

G. F. Bertsch†

Lawrence Berkeley Laboratory, Berkeley, California 94720

(Received 20 September 1976)

Pion production from heavy-ion collisions is calculated in the independent-particle model, using nucleon-nucleon cross section data as input information. The assumption is made that only the first collision of a nucleon pair can create a pion, and also all collective effects are neglected. For the representative case of ^{16}O bombardment of ^{238}U at 250 MeV/nucleon, one out of seven inelastic collisions should produce a pion. One-third of these pions should be able to escape to the outside. The pion spectrum peaks at 20 MeV with an average energy of 50 MeV, viewed in the nucleon-nucleon center-of-mass frame.

[NUCLEAR REACTIONS Pion production in heavy-ion collisions, calculate σ ,
 $\sigma(E_\pi)$.]

I. INTRODUCTION

The energy range 100–300 MeV/nucleon in heavy-ion collisions is interesting because while the energy is high enough to allow strong interpenetration of the nuclei, with a density increase of a factor of 2, it is still low enough that collective effects associated with the higher density might have a chance to manifest themselves. As it happens, this energy region encompasses the threshold for significant pion production. Of the observable effects that can be easily measured, the pion production cross section at threshold is particularly sensitive to collective phenomena. The purpose of this paper, however, is to calculate the pion production with the most economical theoretical assumptions and, in particular, with no collective effects at all. This model could provide a baseline for theoretical discussions of experiments: Discrepancies by orders of magnitude one way or the other would provide an indication of various possible collective effects.

Our picture of the threshold production is that the Fermi momentum of the two nuclei combine to permit pion-producing nucleon-nucleon collisions. However, the initial distribution of nucleons in momentum space rapidly degrades to a thermal distribution, which is much less favorable for producing pions. The created pions have a relatively long mean free path (~ 5 fm) and thus provide a probe of the nuclear interior at the initial stages of collision.

Following this picture, we need the following ingredients for the calculation: first, the initial distribution of nucleons in phase space; second, the total nucleon-nucleon cross sections in order to calculate the rate of depletion of nucleons from the initial distribution; and, finally, the pion production cross sections for nucleon-nucleon collisions.

We shall neglect the possibility of pion production after the initial collision of a nucleon. Consequently, the calculation will be unreliable at higher energies.

To gain some perspective, we can view this model as a simple approximation to the solution of the classical Boltzmann equation for the particles. Our model contains all the assumptions of incoherence built into the Monte Carlo statistical cascade calculations of pion production by protons^{1,2} as well as the further assumption that only the first collision is important. We now examine the various ingredients of the model in detail.

NUCLEON DISTRIBUTION FUNCTION

For individual nuclei, we assume the distribution function of the Fermi gas model, specifically

$$f(p, \nu) = \rho(\nu) \theta(|p| - p_F) / (4\pi p_F^3 / 3). \quad (1)$$

This model differs in the surface region from the more customary Thomas-Fermi approximation, which utilizes a local Fermi momentum depending on position. The ansatz Eq. (1) is easier to apply than the Thomas-Fermi approximation, because the spatial dependence is separable from the momentum dependence.

Before proceeding, it would be useful to have a gauge of reliability of the Fermi gas approximation. A good test is provided by the response function, which is simply the probability of exciting the nucleus as a function of energy and momentum transfer. Threshold pion production by two nuclei requires a large momentum transfer to each nucleus with only small excitation energy. In the Fermi gas model, this restricts momentum transfers to around $2k_F \sim 2.5 \text{ fm}^{-1}$. Experimentally, the response to electrons has been measured near this

momentum transfer.³ The analysis in Ref. 3 shows that a modified Fermi gas model works quite well for describing the total inelastic strength. The portion of the strength function at lowest energies could easily be in error by a factor of 2, however. This is also evident in the comparison of the random-phase approximation theory with the Fermi gas model at momentum transfer of 0.8 fm^{-1} .⁴ In the threshold production of antinucleons, the Fermi gas model proves to be inadequate,⁵ but this reaction requires momentum transfers near 10 fm^{-1} , which is far from the allowed region in the Fermi gas model.

When the two nuclei merge, the distribution function in momentum space will be described by two (possibly intersecting) spheres. This distribution function can be compared with that predicted by Hartree-Fock theory of semi-infinite slabs. When the two slabs collide, a high density region will be formed, separated from the region of impinging nuclear matter by a transition region. Let us choose the direction of motion along the z axis. Then only the z component of the nucleon momentum can change in the collision. If the width of the transition region is not too small, nucleons at the point (p_z, p_x, p_y) in momentum space are moved to the point (p'_z, p_x, p_y) on the high density side of the collision, where p'_z is related to p_z by

$$(p'_z + mv)^2 = (p_z + mv)^2 + 2m\Delta V. \quad (2)$$

Here v is the velocity of the transition region, and ΔV is the change in the single-particle potential from the low density to high density region. The actual geometry of the Fermi surface is thus two (possibly intersecting) spheroids.

It is reasonable to replace these spheroids by spheres, leaving the geometry characterized by the separation of the centers of the two spheres, P . To relate this geometry to the initial conditions characterized by a bombarding energy, a theory of nuclear matter compressibility is need-

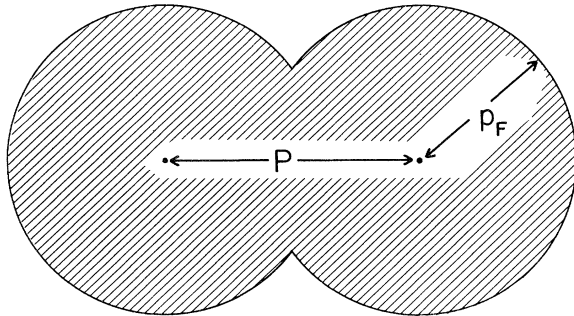


FIG. 1. Geometry of the double Fermi sphere for $P = 1.64p_F$, corresponding to a collision with $E_{\text{lab}} = 100 \text{ MeV/nucleon}$.

ed. In what follows, we shall assign incident energies assuming that $\Delta V = 0$, in which case the displaced Fermi spheres of the two colliding nuclei become superimposed without distortion during the collision. This assumption requires the nuclei to be extremely soft. The Brueckner calculations of Negele, reported in Ref. 6, have $\Delta V = 0$ for a 70% increase in density, from 0.16 to 0.27 fm^{-3} , and $\Delta V = 80$ for a density doubling. The popular Hartree-Fock theories based on the Skyrme parametrization of the interaction are somewhat stiffer, with $\Delta V = 120 \text{ MeV}$ for density doubling. These numbers give an idea of possible shifts in energy scales resulting from the actual Hartree-Fock dynamics.

NUCLEON-NUCLEON COLLISIONS

The initial sharp distribution function of two spheres will be degraded by the nucleon collisions to an isotropic distribution characterized by a temperature. We focus our attention on the regions of highest relative momentum, the endcaps of the initial distribution, and will neglect the possibility of pion production by a nucleon which has already been knocked out of the endcap. To compute the decay rate of the endcaps, we define an effective cross section for the scattering of a nucleon p_1 in an endcap with another nucleon,

$$\sigma_{\text{eff}}^N(p_1) = \int \frac{d^3 p_2}{4\pi p_F^3/3} \frac{p_2 - p_1}{P} \frac{\sigma_{pp}(E) + \sigma_{np}(E)}{2} \frac{\Omega}{4\pi}, \quad (3)$$

where E is the energy of the nucleon-nucleon collision corresponding to relative momentum $\frac{1}{2}(p_2 - p_1)$, and Ω is the solid angle of final states permitted by the Pauli principle,

$$\Omega = \int d\hat{n} \prod_i \theta(p^i - p_F) \quad (4)$$

with $p^i = \frac{1}{2} |p_1 + p_2 \pm \hat{n} |p_1 - p_2| \pm P|$. We evaluate Eq. (3) with the nuclear cross sections of Ref. 2. The results are given in Table I for the case with $p_1 = (p_F, 0, 0)$. The decay rate of the endcap is given by

$$\frac{1}{\tau} = \sigma \rho \frac{P}{m}. \quad (5)$$

Using $p_F/m = 0.28c$ and $\rho = 0.16 \text{ fm}^{-3}$, we compute the decay time τ in Table II. It is interesting to compare this decay time with the corresponding quantity for a single nucleon outside a Fermi sphere. If the cross section is assumed constant, this rate can be computed analytically.^{7,8} The results with the same cross sections as used previously, but using only a single sphere exclusion, are given in Table II. There is not much difference for $P \sim p_F$ and larger, but for small p the difference

TABLE I. Effective collision cross section for a nucleon in a distorted Fermi sea to scatter from other nucleons in the Fermi sea, from Eq. (3). The Fermi sea is bounded by two spheres of radius $p_F = 1.34 \text{ fm}^{-1}$, separated by momentum P . In the second column is given the density of nuclear matter with this geometry of the Fermi sea, in terms of $\rho_0 = (2/3\pi^2)p_F^3$. The third column gives the effective cross sections for nucleons at the top of the Fermi sea, $p = p_F + \frac{1}{2}P$. The fourth column gives effective cross section for nucleons somewhat deeper, $p = 0.65p_F + \frac{1}{2}P$.

| P/p_F | ρ/ρ_0 | $\sigma_{\text{eff}}^N(p_F + \frac{1}{2}P)$ (mb) | $\sigma_{\text{eff}}^N(0.65p_F + \frac{1}{2}P)$ (mb) |
|---------|---------------|---|---|
| 0.05 | 1.04 | 0.4 | |
| 0.1 | 1.07 | 1.0 | |
| 0.2 | 1.15 | 2.1 | |
| 0.3 | 1.22 | 3.3 | |
| 0.5 | 1.49 | 6.5 | |
| 1.0 | 1.69 | 15 | |
| 1.64 | | | 15 |
| 2.0 | 2 | 33 | 21 |
| 2.28 | | | 23 |
| 2.55 | | | 26 |
| 2.77 | | | 27 |
| 3.0 | 2 | 40 | |
| 4.0 | 2 | 49 | |

in exclusion makes more than an order of magnitude difference in decay rate.

The pion production threshold in the Fermi gas model is at $P = 1.18p_F$, corresponding to an incident energy of 54 MeV/nucleon in the $\Delta V = 0$ model. The combination of Fermi momenta of the nucleons gives enough energy to create pions at even lower energies; it is exclusion of final state phase space that determines this threshold.

To calculate the rate of pion production from nucleon-nucleon cross sections, we shall have to make some assumption about the final state phase

TABLE II. Decay times for endcaps of double sphere distribution function, from Eq. (5). In the last column is given the decay time for a single nucleon outside a Fermi sphere, having momentum $p_F + P$.

| P/p_F | τ (double sphere) (fm/c) | τ (single nucleon) (fm/c) |
|---------|----------------------------------|-----------------------------------|
| 0.05 | 10^4 | 230 |
| 0.1 | 2×10^3 | 63 |
| 0.2 | 500 | 20 |
| 0.3 | 220 | 11 |
| 0.5 | 70 | 6.8 |
| 1.0 | 15 | 4.8 |
| 2.0 | 3.3 | 3.1 |
| 3.0 | 1.8 | 1.7 |
| 4.0 | 1.1 | 1.1 |

TABLE III. Effective π production cross sections from nucleon distribution of two spheres separated by a momentum P . The values for the lab energy of the projectile assume that $\Delta V = 0$ in the Hartree-Fock theory.

| P/p_F | E_{lab} (MeV) | σ_{eff} (mb) |
|---------|------------------------|----------------------------|
| 1.34 | 70 | 2×10^{-6} |
| 1.64 | 100 | 0.002 |
| 1.98 | 150 | 0.04 |
| 2.28 | 200 | 0.19 |
| 2.55 | 250 | 0.57 |
| 2.77 | 300 | 1.2 |
| 3.94 | 700 | 9.5 |

space. As was done in Eq. (4), we shall assume that the reaction cross section is strictly proportional to phase space, and weight the total production rate by the fraction of phase space available in the nuclear medium. Thus an effective pion production cross section is defined,

$$\sigma_{\text{eff}}^{\pi} = \int \frac{d^3 p_1}{(4/3)\pi p_F^3} \frac{d^3 p_2}{(4/3)\pi p_F^3} \times \sigma_{\pi}(E) \frac{p_1 - p_2}{P} \left(\frac{p+n \text{ phase space in medium}}{p+n \text{ free phase space}} \right). \quad (6)$$

The effective cross sections are reported in Table III.

The input pion production cross sections were abstracted from the compilation of Barashenkov and Maltsev,⁹ and are quoted in Table IV. These cross sections are for collisions between identical nucleons. The $n+p$ cross section is assumed to be half the $p-p$ cross section, which follows if production takes place only between pairs with isospin $T = 1$.

This model cannot be correct at the lowest energies, because the lowest energy production is not to continuum $n+p$ states, but mostly to the deuteron final states. However, the major con-

TABLE IV. Pion production cross sections from $p-p$ scattering, from Barashenkov and Maltsev (Ref. 9). E_{kin} labels the kinetic energy in final state, $\pi^+ + n + p$.

| E_{kin} (MeV) | σ (mb) |
|------------------------|---------------|
| 23 | 0.55 |
| 41 | 1.85 |
| 67 | 2.43 |
| 88 | 3.8 |
| 99 | 5.9 |
| 121 | 8.8 |
| 143 | 12.4 |
| 161 | 16 |
| 224 | 25 |

tribution to the integral (6) comes from nucleon pairs with energies well above this low energy region.

In the case of $P=2.55$, corresponding to 250 MeV/nucleon lab energy, we examine the production in more detail. The most important region of the initial nucleon distribution is in the vicinity of $p_z \approx \frac{1}{2}P + 0.65p_F$. Thus the picture that the endcaps dominate the production is quite justified. The spectrum of energies of the pions produced in the nuclear medium is given in Fig. 2. The distribution is given in the nucleon-nucleon center-of-mass frame, i.e., a frame moving with velocity of $0.34c$. The pions tend to be of very low energy in this frame, with median energy near 50 MeV. There is enough energy available in nucleon pairs to produce pions with kinetic energies up to 250 MeV, but the phase space favors very low energy. The angular distribution would be strongly peaked along the beam axis following the nucleon-nucleon production cross section.¹⁰ This, of course, neglects inelastic scattering of the pions on the way out of the nucleus.

PRODUCTION RATES

We are now ready to compute the pion production rate. We idealize a collision to that of two semi-infinite slabs, impinging on each other with a relative velocity v , with the surfaces coming into contact at $t=0$ and $z=0$. The nucleon distribution function of the endcaps in the overlap region decays at a rate

$$\exp\left[-\left(\frac{1}{2}vt \pm z\right)\sigma^N \rho_0\right] \begin{cases} + & \text{for } p_z > 0, \\ - & \text{for } p_z < 0 \end{cases}$$

and the pion production rate, per unit volume, is

$$\frac{dn_\pi}{dt} = v\sigma^\pi \exp\left[-\left(\frac{1}{2}vt + z\right)\sigma^N \rho_0\right] \exp\left[-\left(\frac{1}{2}vt - z\right)\sigma^N \rho_0\right] \times \rho\left(\frac{1}{2}vt + z\right)\rho\left(\frac{1}{2}vt - z\right). \quad (7)$$

This may be integrated over space to obtain the production rate per unit area,

$$\frac{dN}{dt dA} = v^2 t \sigma_\pi \rho_0^2 \exp(-vt\sigma^N \rho_0). \quad (8)$$

Integrating this over time we have for the number of pions produced,

$$N = \frac{\sigma^\pi}{(\sigma^N)^2} A, \quad (9)$$

where A is the collisional area. This simple formula can be understood as follows: The number of pions produced is the product of the probability of an individual nucleon producing a pion, σ^π/σ^N , multiplied by the number of nucleons which can make an initial collision, A/σ^N .

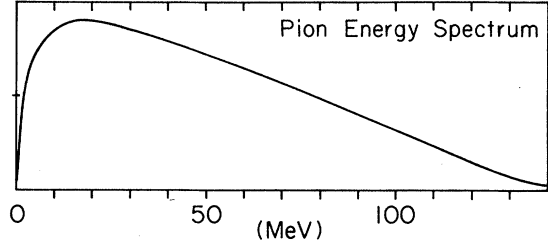


FIG. 2. The energy spectrum of pions produced by nucleon-nucleon collisions in the double Fermi sphere with $P=2.55p_F$. The reference frame is moving with velocity equal to $0.34c$.

How far do the nuclei overlap when the pions are produced? The mean overlap can be computed as

$$\int \frac{vt(dN/dt)dt}{N} = \frac{2}{\sigma^N \rho_0} \approx 4 \text{ fm for } P=2.5. \quad (10)$$

This overlap is quite substantial: Pion production should sample a dense nuclear interior.

To make a concrete example, let us consider the collision of ^{16}O on ^{238}U . Considering each of these nuclei to be a sphere uniformly filled to a density 0.16, the radii are $R_0=2.9$ and $R_U=7.1$ fm. The area of the collision we take to be the area of overlap of the two nuclei, viewed along the collision axis. The formula (9) will then be an overestimate, because the oxygen nucleus is thinner on the edges than the 4 fm required to reach mean penetration for pion production. Averaging the area over impact parameters,

$$A = \int_0^{R_0+R_U} \frac{bdb}{\frac{1}{2}(R_0+R_U)^2} \times \int d^2r \theta(R_0 - |r|) \theta(R_U - |r-b|). \quad (11)$$

we determine an average area per inelastic collision to be 13 fm^2 . Replacing the sharp-edged distribution by a realistic diffuse distribution would increase the inelastic cross section by 20%, according to unpublished calculations of Dover and

TABLE V. Probability of pion production for inelastic collisions of ^{16}O on ^{238}U . For pions observable in the laboratory, these numbers should be multiplied by the probability of escape, $\sim \frac{1}{3}$.

| P/p_F | E_{lab} (MeV) | N_π [Eq. (9)] | Thermal model | |
|---------|------------------------|-------------------|---------------|-------------|
| | | | T (MeV) | N_π |
| 1.64 | 100 | 1/1000 | 25 | 1/3000 |
| 1.98 | 150 | 1/80 | | |
| 2.28 | 200 | 1/20 | 39 | 1/50 |
| 2.55 | 250 | 1/9 | | |
| 2.77 | 300 | 1/5 | 54 | |
| | 2000 | | 146 | 8 (Ref. 11) |

Vary. Substituting in Eq. (9), the average number of pions produced per inelastic collision is given in Table V. For this computation we used the effective nucleon scattering cross sections for nucleons at momentum $\frac{1}{2}P + 0.65p_F$, quoted in the last column of Table I.

Another model for pion production is the statistical model, in which thermal equilibrium is assumed over some region of space, and the equilibrium number of pions calculated. This model has been applied for high energy heavy ion collisions, assuming all the energy is equilibrated in a nuclear volume.¹¹ This model has also been applied for lower energies, assuming one-dimensional shock formation, and consequent high compressions.¹² We compare our results with the more conservative model, which assumes that all of the energy is available in the nucleon-nucleon center-of-mass system is deposited in a volume equal to the volume of maximum overlap of the two ions. Averaging over impact parameter, this volume can be taken as

$$v = \frac{4\pi R_0^3}{3} \frac{\langle A \rangle}{\pi R_0^2}. \quad (12)$$

The number of pions is then given by the product of the density in the Bose-Einstein distribution and the volume. The temperature is calculated using the Fermi-Dirac distribution for the nucleons and requiring energy conservation. The results are given in the last two columns of Table V. We see that at low energies, thermal production is less favorable than first-collision production, justifying our approximation.

Finally, we must determine the probability for the created pions to escape from the collision region. This requires knowledge of the mean free path, which unfortunately is not well determined experimentally for low energy pions. However, there are several independent threads of evidence, including a measurement of the absorption rate of 130 MeV pions,¹³ an analysis of pion production from proton-nucleus collisions,² which point to a mean free path of about 5 fm.¹⁴ The average depth at which a pion is produced in our example of ^{16}O on ^{238}U is about one mean free path. Thus, we expect one out of three of the pions produced to emerge from the collision. The number in Table

V should then be divided by three to obtain production rates of laboratory pions.

Although the experimental evidence on pion production by heavy ions is meager, a few words on experimental results are in order. The kind of model we consider is quite successful for describing pion production from proton induced collisions at higher energies.² There is low energy data for production from proton collisions,¹⁵ with cross sections in the microbarn range. The present model can be applied to proton collisions by replacing the double sphere geometry by a particle outside a single Fermi sphere. The momentum of the particle is set by energy conservation with $\Delta V = -45$. This model gives the correct order of magnitude for the total cross section observed in Ref. 15.

Among experiments studying pion production by complex projectiles, the lowest energy data are with 70 MeV/nucleon ^3He ions. The cross section for pion production is less than a nanobarn.¹⁶ The present model gives zero if the internal momentum of the ^3He is neglected, and ~ 1 nb if the ^3He is treated as a Fermi sea with the usual Fermi momentum. At 280 MeV/nucleon incident energy, ^{20}Ne projectiles have been used in a photographic emulsion experiment.¹⁷ Roughly one candidate pion track is observed per inelastic collision. This is a very large production rate, and if confirmed would indicate that coherent mechanisms come into play. At bombarding energies of 500 MeV/nucleon and higher, the heavy ion production rate is similar to the single nucleon production rate, although some difference is seen in the cross section for pions of especially high momentum.^{20,21}

It is easy to imagine improvements of the model to include collective effects. The free particle kinematics for the collisions can be replaced by kinematics in the medium, with a different relation between momentum and energy of the particles. In an extreme case, this would allow pion production by single nucleons rather than pair collisions. This mechanism has been discussed by Sawyer.¹⁸ It has also been suggested that collective instabilities of the distorted Fermi surface would lead to faster equilibration.¹⁹ This would imply a lower pion production rate in our model.

The author acknowledges helpful conversations with J. Hüfner.

*Work supported under the auspices of the U. S. ERDA.

†Permanent address: Physics Department, Michigan State University, East Lansing, Michigan 48824.

¹N. Metropolis *et al.*, Phys. Rev. **110**, 204 (1958).

²D. Sparrow *et al.*, Phys. Rev. C **10**, 2215 (1974).

³E. Moniz *et al.*, Phys. Rev. Lett. **26**, 445 (1971).

⁴G. F. Bertsch and S. F. Tsai, Phys. Rep. C **18**, 126 (1975).

⁵P. Piroué and A. Smith, Phys. Rev. **148**, 1315 (1966).

⁶J. W. Negele and D. Vautherin, Phys. Rev. C **5**, 1472

- (1972).
- ⁷K. Kikuchi and M. Kawai, *Nuclear Matter and Nuclear Reactions* (North-Holland, Amsterdam, 1968).
- ⁸V. M. Galitskii, *Zh. Eksp. Teor. Fiz.* 34, 151 (1958) [*Sov. Phys.-JETP* 7, 104 (1958)].
- ⁹V. Barashenkov and V. Maltsev, *Fortschr. Phys.* 9, 553 (1961).
- ¹⁰C. Richard-Serre *et al.*, *Nucl Phys.* B20, 413 (1970).
- ¹¹G. Chapline *et al.*, *Phys. Rev. D* 8, 4302 (1973).
- ¹²Y. Kitazoe, K. Matsuoka, and M. Sano, *Prog. Theor. Phys.* 56, 860 (1976).
- ¹³E. Belotti *et al.*, *Nuovo Cimento* 18A, 75 (1973).
- ¹⁴J. Hüfner, *Phys. Rep.* C21, 1 (1975).
- ¹⁵S. Dahlgren, B. Hoisted, and P. Grafstrom, *Phys. Lett.* 35B, 219 (1971).
- ¹⁶N. Wall *et al.*, *Nucl. Phys.* A268, 459 (1976).
- ¹⁷P. McNulty and R. Filz, in *Proceedings of the Conference on Nuclear Photography and Solid State Track Detectors*, edited by M. Nicolae (Institute of Atomic Physics, Bucharest, 1972), Vol. II, p. 170.
- ¹⁸R. Sawyer (unpublished).
- ¹⁹V. Ruck, M. Gyulassy, and W. Greiner, *Z. Phys.* A277, 391 (1976).
- ²⁰K. G. Vosburgh *et al.*, *Phys. Rev. D* 11, 1743 (1975).
- ²¹J. Papp *et al.*, *Phys. Rev. Lett.* 34, 601 (1975).